Note

Low Atmospheric Oxygen Attenuates Alpha Oscillations in the Primary Motor Cortex of Awake Rats

Masashi Kawamura,[a] Airi Yoshimoto,[a] Yuji Ikegaya,[a,b,c] and Nobuyoshi Matsumoto*[,a,b]

[a] *Graduate School of Pharmaceutical Sciences, The University of Tokyo, 7–3–1 Hongo, Bunkyo-ku, Tokyo 113–0033, Japan:* [b] *Institute for AI and Beyond, The University of Tokyo, 7–3–1 Hongo, Bunkyo-ku, Tokyo 113–0033, Japan: and* [c] *Center for Information and Neural Networks, National Institute of Information and Communications Technology, 1–4 Yamadaoka, Suita, Osaka 565–0871, Japan.*

Received December 7, 2023; accepted January 18, 2024

Oxygen is pivotal for survival of animals. Their cellular activity and cognitive behavior are impaired when atmospheric oxygen is insufficient, called hypoxia. However, concurrent effects of hypoxia on physiological signals are poorly understood. To address this question, we simultaneously recorded local field potentials in the primary motor cortex, primary somatosensory, and anterior cingulate cortex, electrocardiograms, electroolfactograms, and electromyograms of rats under acute hypoxic conditions (*i.e.*, 5.0% O_2). Exposure to acute hypoxia significantly attenuated alpha oscillations alone in the primary motor cortex, while we failed to find any effects of acute hypoxia on the oscillatory power in the somatosensory cortex or anterior cingulate cortex. These area- and frequency-specific effects by hypoxia may be accounted for by neural innervation from the brainstem to each cortical area *via* thalamic relay nuclei. Moreover, we found that heart rate and respiratory rate were increased during acute hypoxia and high heart rate was maintained even after the oxygen level returned to the baseline. Altogether, our study characterizes a systemic effect of atmospheric hypoxia on neural and peripheral signals from physiological viewpoints, leading to bridging a gap between cellular and behavioral levels.

Key words alpha oscillation, motor cortex, rat, hypoxia, local field potential

INTRODUCTION

Sufficient oxygen is essential for biological activity and survival of animals. Once oxygen is not fully supplied to cells and tissues of an animal, their functions are impaired by insufficient oxygen. At the cellular level, ventilatory, hematological, cardiovascular, and metabolic parameters are affected by low concentrations of atmospheric oxygen, called hypoxia.[1–3] Moreover, cognitive performance is also impaired by chronic hypoxia.[4,5] To bridge the gap between cellular and cognitive functions, another physiological study monitored electroencephalograms of rats under high-altitude conditions to investigate the effects of hypobaric hypoxia on neural activity and revealed that neural activity was shifted from fast to slow oscillations.[6] However, the possibility that this reorganization of oscillatory frequencies in neural activity is caused by the change in total air pressure cannot be excluded and is yet to be addressed. To evaluate a net effect of oxygen concentration in air on neural and peripheral activity, we devised an experimental configuration in which oxygen concentration levels were exclusively manipulated while the total atmospheric pressure was maintained at the standard 1 atm, which we call 'experimental hypoxia,' hereafter. We recorded local field potentials (LFPs) in the primary motor cortex (M1), primary somatosensory cortex (S1), and anterior cingulate cortex (ACC) as well as electrocardiograms (ECGs), electroolfactograms (EOGs), and electromyograms (EMGs) of rats acutely exposed to the experimental hypoxia to monitor neural and cardiopulmonary activity. We analyzed the neural signals in a frequency domain using the fast Fourier transform (FFT), and evaluated heart rate (HR), heart rate variability (HRV), and breathing rate (BR) based on ECGs and EOGs.

MATERIALS AND METHODS

Ethical Approvals Animal experiments were performed with the approval of the Animal Experiment Ethics Committee at the University of Tokyo (Approval Number: P4-14) and according to the University of Tokyo guidelines for the care and use of laboratory animals. These experimental protocols were carried out in accordance with the Fundamental Guidelines for the Proper Conduct of Animal Experiments and Related Activities of the Academic Research Institutions (Ministry of Education, Culture, Sports, Science and Technology, Notice No. 71 of 2006), the Standards for Breeding and Housing of and Pain Alleviation for Experimental Animals (Ministry of the Environment, Notice No. 88 of 2006) and the Guidelines on the Method of Animal Disposal (Prime Minister's Office, Notice No. 40 of 1995). While our experimental protocols have a mandate to humanely euthanize animals if they exhibit any signs of pain, prominent lethargy, and discomfort, such symptoms were not observed in any of the rats tested in this study. All efforts were made to minimize the animals' suffering.

Animals A total of nine male 14- to- 16-week-old Wistar rats (Japan SLC, Japan) were housed individually under conditions of controlled temperature and humidity (22 ± 1 °C, 55 ± 5%) and maintained on a 12/12-h light/dark cycle (lights off from 7:00 a.m. to 7:00 p.m.) with *ad libitum* access to food and water. Rats were habituated to experimenters by daily handling.

Preparation A recording interface assembly was prepared

* To whom correspondence should be addressed. e-mail: nobuyoshi@matsumoto.ac

as previously described.[7–12] In short, the assembly was composed of an electrical interface board (EIB) (EIB-36-PTB, Neuralynx, U.S.A.) and shell and core bodies custom-made by a 3-D printer. The EIB had a sequence of metal holes for connections with wire electrodes. A given individual hole was conductively connected with one end of the insulated wire (approx. 5 cm) using attachment pins, whereas the opposite end was soldered to a corresponding individual electrode during surgery.

Surgery The basic procedure of the following stereotaxic surgery in accordance with our previous literature.[10–14]

General anesthesia was induced in the rats and maintained with 2–3 and 1–2% isoflurane gas, with careful inspection of the animal's condition during the whole surgical procedure. Veterinary ointment was applied to the rat's eyes to prevent drying. The skin was sterilized with 70% ethanol whenever an incision was made.

After complete anesthesia was confirmed, electrodes for ECGs and EMGs were implanted as described previously.[7] Briefly, a rat was placed on its back, after which one wire electrode (AS633, Cooner Wire, CA, U.S.A.) was attached to the pectoralis muscle to record ECGs. The rat was then turned over, laid on its stomach, and mounted onto a stereotaxic apparatus (SR-6R-HT, Narishige, Japan).[10] Another wire electrode (AS633, Cooner Wire) was implanted into the trapezius to record EMGs. The scalp was then removed with a surgical knife. Circular craniotomies with a diameter of approximately 0.9 mm were performed using a high-speed dental drill (SD-102, Narishige). Epidural stainless-steel screws (1.4 mm in diameter, 3.0 mm in length) were used to record LFPs from M1 and S1, whereas smaller screw electrodes (1.0 mm in diameter, 4.0 mm in length) were used to record LFPs from ACC (Figs. 1A, B). The three screw electrodes were stereotaxically implanted unilaterally into M1 (3.2 mm anterior and 3.0 mm lateral to bregma), S1 (2.1 mm posterior and 2.8 mm lateral to bregma), and ACC (3.0 mm anterior and 0.5 mm lateral to bregma) (Fig. 1B). Two stainless-steel screws were additionally implanted into the bone above the cerebellum (9.6 mm posterior and 1.0 mm bilateral to bregma) as ground and reference electrodes. Each of the open edges of electrodes was soldered to the corresponding open edge of insulated wires of the recording interface assembly. To record electroolfactograms (EOGs) indicative of respiratory signals, a small hole was drilled above the anterior portion of the nasal bone (3.0 mm anterior to the nasal fissure and 0.5 mm lateral to bregma) until the olfactory epithelium was exposed.[15] One wire electrode (AS633, Cooner Wire) was inserted inside the soft epithelial tissue. For each of wire electrodes to record ECGs, EMGs, and EOGs, the insulation was removed from the wire tip and the other end was connected to the same assembly as the rest of the electrodes. This assembly including all electrodes was secured to the skull using dental cement.

Following surgery, each rat was allowed to recover from

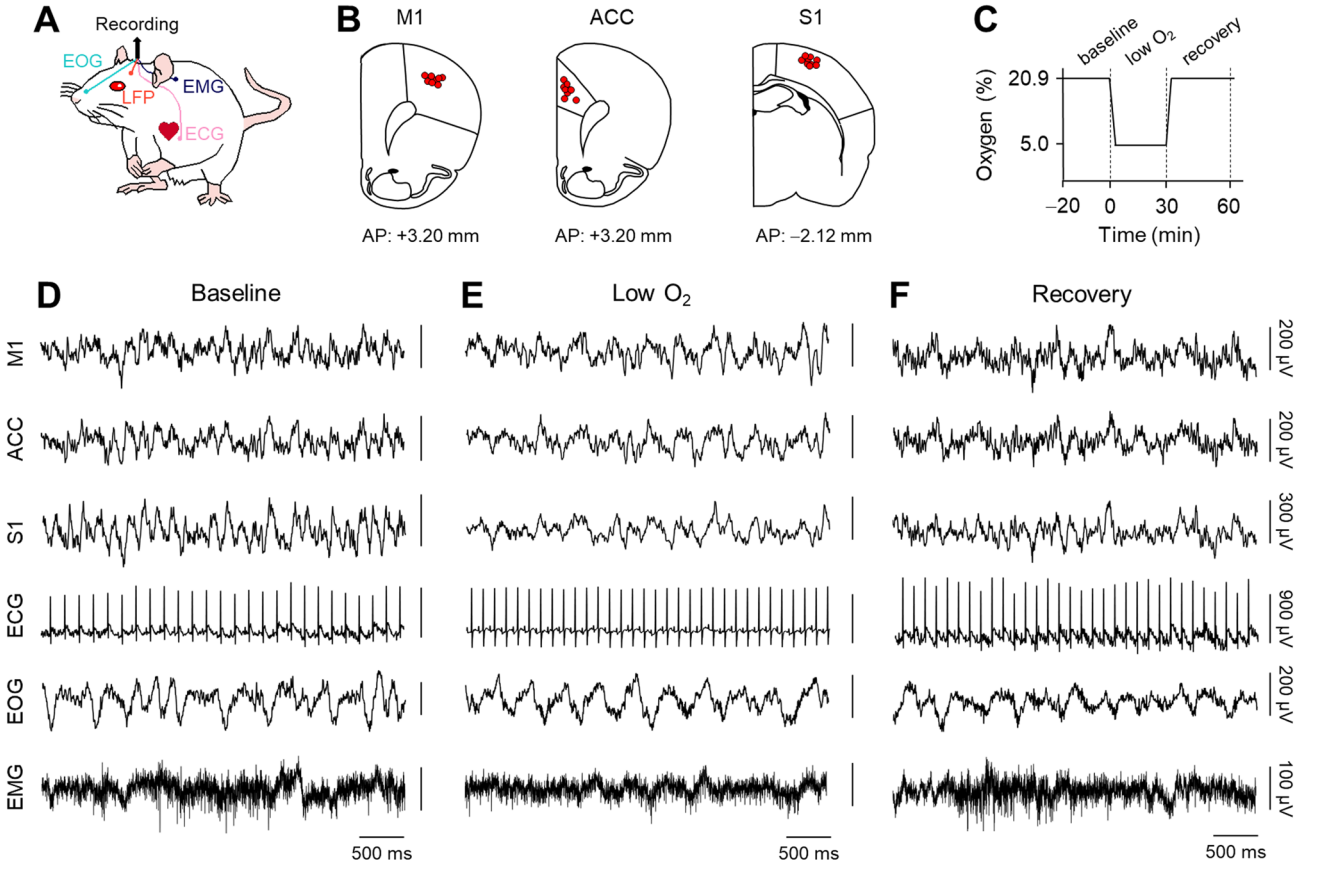

Fig. 1. Simultaneous Recording of LFPs, ECGs, EOGs, and EMGs of Rats before, during, and after the Experimental Hypoxia

A, Schematic of recording systems. **B**, *Post-hoc* verification of the sites (*red*) of recording electrodes in M1 (*left*), ACC (*middle*) and S1 (*right*) superimposed on a simplified brain atlas ($n = 9$ rats). **C**, Time course of oxygen concentrations in air. $Time = 0$ (min) denotes the onset of experimental hypoxia, which is terminated at $Time = 30$. Baseline, low O_2, and recovery periods are defined as $-20 < Time < 0$, $0 < Time < 30$, $30 < Time < 60$, respectively. **D**, Representative traces of LFPs in M1 (*first* (*topmost*)), ACC (*second*), S1 (*third*), ECGs (*fourth*), EOGs (*fifth*), and EMGs (*sixth*) during the baseline period. **E**, **F**, Same as D, but during the low O_2 and recovery periods, respectively. Abbreviations: LFP, local field potential; EOG, electroolfactogram; EMG, electromyogram; ECG, electrocardiogram; M1, primary motor cortex; ACC, anterior cingulate cortex; S1, primary somatosensory cortex; AP, anterior-posterior.

anesthesia and was housed individually with free access to water and food. For the first few days after surgery, the health condition of animals was carefully checked every 3 h except during the night (*i.e.*, 8:00 p.m. to 8:00 a.m.).

Recording System A plastic cage for rearing was modified for electrophysiology (see the next section) as follows. Two opposite walls of the cage were perforated. Two small holes on one side wall were connected to gas cylinders (for oxygen and nitrogen) through two conduits, whereas a hole on the other side was attached to a suction pump *via* another tube. Flow rates of oxygen and nitrogen gases were meticulously regulated by experimenters using dedicated regulators. An oxygen sensor was suspended from the ceiling of the cage and connected to an oxygen meter (JKO-25Ver3, Ichinen Manufacturing, Japan) through a hole on the ceiling. The oxygen sensor and meter were further connected to a data acquisition system (CerePlex Direct, Blackrock Neurotech, U.S.A.; see the next section for details) *via* a cable (AOUT-JKOV3, Ichinen Manufacturing).

After rats were acclimated to the recording cage for 20 min, the concentration of oxygen in the cage was monitored using the oximeter and carefully maintained at normoxic 20.9% through continuous ventilation during a 'baseline' period lasting 20 min. After the 20-min baseline period, flow rates of oxygen and nitrogen were manually controlled so that the oxygen levels could be decreased to approximately 5.0% and maintained for 30 min (named a 'low O_2' period). Following the low O_2 period, the recording cage was depressurized using a suction pump, so that air came into the cage through a hole on the ceiling and circulated. The oxygen levels were quickly returned to 20.9% and kept constant for at least 30 min (named a 'recovery' period). The onset of the low O_2 period was defined as $Time = 0$ (min) (Fig. 1C).

The recording cage was filled with oxygen and nitrogen alone; the nitrogen levels were approximately 79.1 and 95.0% when the oxygen levels were 20.9 and 5.0%. The carbon dioxide level in the recording cage was presumed infinitesimally close to zero; however, note that the nitrogen and carbon dioxide levels were not directly measured using sensors.

***In Vivo* Electrophysiology** After full recovery from surgery, the animals were habituated to the apparatus for at least 2 d.

The EIB of the recording interface assembly was connected to a digital headstage (CerePlex M, Blackrock Neurotech), and the digitized signals were amplified and transferred to the data acquisition system (CerePlex Direct, Blackrock Neurotech).[7,16] Electrophysiological signals were digitized at a sampling rate of 2 kHz. LFPs, ECGs, EMGs, and EOGs were first recorded for 20 min during the baseline period (Fig. 1D). After the baseline period, oxygen levels were manually dropped off to 5%, and electrophysiological signals were recorded for 30 min during the low O_2 period and further for 30 min during the recovery period (Figs. 1E, F).

The experimenters carefully monitored behavior of all rats and confirmed that they were awake during the entire recording period, based on their eyeblink (*i.e.*, eye opening), limb movement, and active whisker deflection.

Histology After the recordings, rats were anesthetized by intraperitoneal injection of an overdose of urethane and transcardially perfused with 0.01 M phosphate-buffered saline (PBS; pH 7.4) and 4% paraformaldehyde (PFA) in 0.01 M PBS, followed by decapitation.[14,17,18] The brains were soaked overnight in 4% PFA for post-fixation and coronally sectioned at a thickness of 100 μm using a vibratome (DTK-1000N, Dosaka EM, Japan).[10,11,19–22] Serial slices were mounted on glass slides and processed for cresyl violet staining.[10–12,14] For cresyl violet staining, the slices were rinsed in water, ethanol, and xylene, counterstained with cresyl violet, and coverslipped with a mounting agent. The positions of all electrodes were confirmed by identifying dents on the neocortical superficial layer or tracks in the subcortical region in the histological tissue. Data were excluded from the subsequent analysis if the electrode position was outside the target brain region. Cresyl violet-stained images were acquired using a phase-contrast microscope (BZ-X710, Keyence, Japan).

Data Analysis All data analyses were performed using custom-made MATLAB routines (MathWorks, U.S.A.). The summarized data in the text are reported as the mean ± the standard deviation. The significance level was set at 0.05, and the null hypothesis was statistically rejected when $p < 0.05$ based on two-tailed tests unless otherwise specified. When multiple pairwise comparisons were required, the significance level was corrected based on *post-hoc* Bonferroni correction.[23]

LFPs and EOGs were converted into a frequency-relevant domain using FFT. The absolute power in specific frequency bands (*i.e.*, delta (0.3–4 Hz), theta (4–8 Hz), alpha (8–15 Hz), beta (15–30 Hz), and gamma (30–90 Hz)) was calculated as the area under the spectra between corresponding frequencies in the frequency domain for each 10-s segment of the recorded data, and then normalized by the absolute power between 0.3–90 Hz. Sixty segments of the normalized power in each frequency band during $-15 < Time < -5$ (min), $20 < Time < 30$ (min), or $40 < Time < 50$ (min) were respectively averaged, and the mean power in the baseline, low O_2, or recovery period was obtained. To display the time course of relative power, the segments of the normalized power were divided by the mean power in the baseline period (Fig. 2A). Moreover, the ratio of the mean power in the low O_2 or recovery period to that in the baseline period was calculated for each frequency band to obtain relative power (Figs. 2B–D). For EMGs, the baseline was first reset to zero (by subtracting the average). The reset EMGs were transformed into absolute values. The absolute values for a 10-s segment were averaged to produce EMG amplitude. The EMG amplitude for each 10-s segment was further processed in the same way as LFPs and EOGs (described above).

BR was quantified based on EOGs using FFT. HR was defined as the inverse of R-R intervals detected in the waveform of ECGs. The root mean square of successive R-R interval differences (*i.e.*, RMSSD) was used as a metric of HRV.[24]

RESULTS

To investigate effects of acute experimental hypoxia on the physiological signals, we designed an experimental setup allowing us to manipulate the oxygen concentration alone with atmospheric oxygen pressure maintained at the standard 1 atm. We recorded LFPs in M1, S1, and ACC as well as EMGs, ECGs, and EOGs of awake rats that acutely experienced experimental hypoxia (Fig. 1, Supplementary Fig. 1).

We calculated the relative power in delta, theta, alpha, beta,

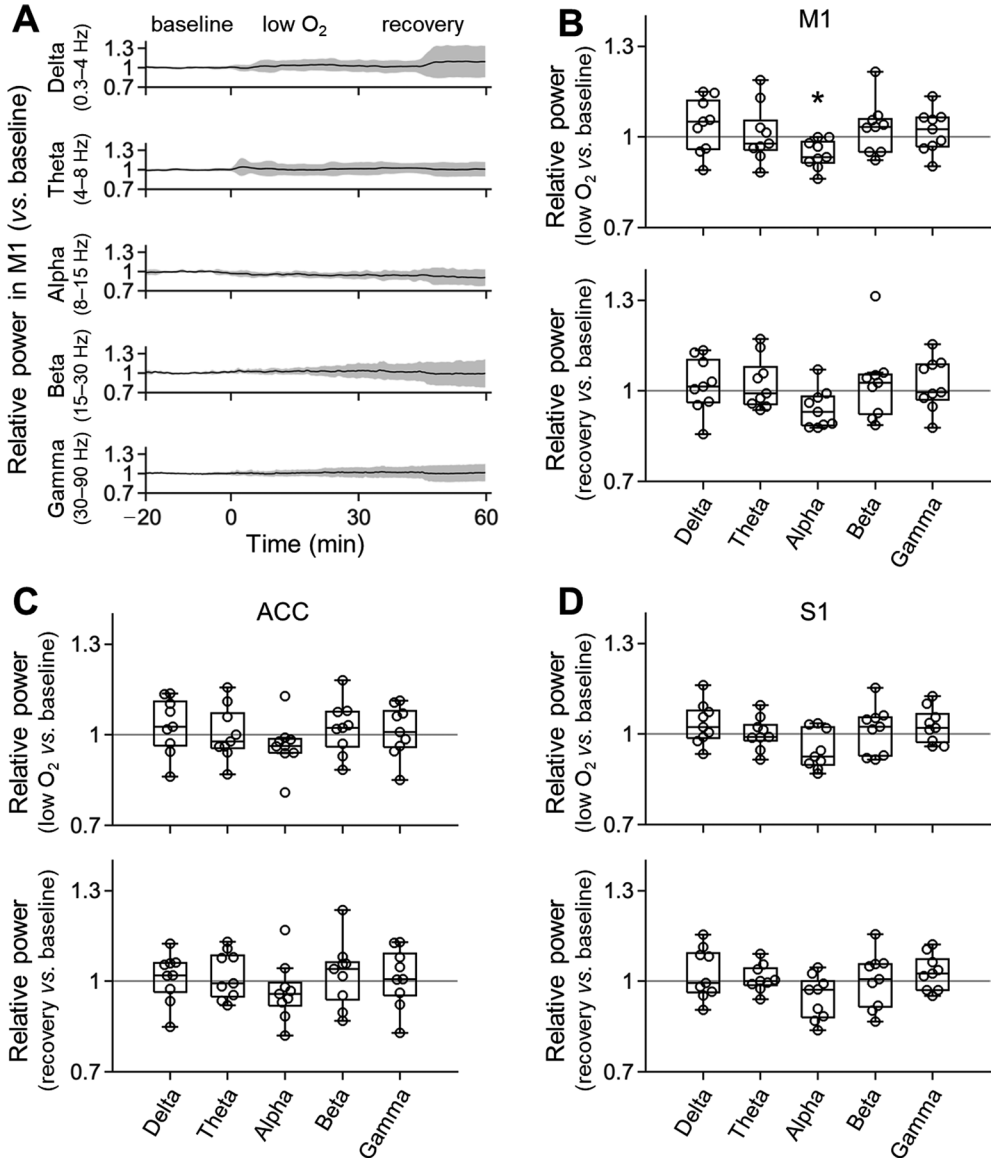

Fig. 2. Effects of Hypoxic Conditions on Cortical Neural Activity

A, Time course of relative power of M1 LFPs in each frequency band (delta (*first*), theta (*second*), alpha (*third*), beta (*fourth*), and gamma (*fifth*)) during the baseline, low O_2, and recovery periods. Data represent the mean (*black*) ± the standard deviation (*gray*) ($n = 9$ rats). **B**, The power of LFPs in each frequency band in M1 during the low O_2 period (*top*) and recovery period (bottom) relative to that during the baseline period. **C**, Same as *B*, but in ACC. **D**, Same as *B*, but in S1. $*p < 0.05/5$; note that the significance level is corrected. *Abbreviations*: LFP, local field potential; M1, primary motor cortex; ACC, anterior cingulate cortex; S1, primary somatosensory cortex.

and gamma frequency bands for the low O_2 and recovery periods for M1, S1, and ACC (see Materials and Methods; Fig. 2A). Compared with the baseline period, the power in alpha oscillations in M1 was significantly decreased in the low O_2 period, but not in the recovery period (P (low O_2, alpha) $= 6.4 \times 10^{-3}$ ($<0.05/5$), $t_8 = 3.66$, $n = 9$ rats, one sample *t*-test *vs.* 1 with the adjusted significance level based on Bonferroni correction; P (recovery, alpha) $= 0.03$ ($>0.05/5$, Bonferroni correction), $t_8 = 2.71$; Fig. 2B), whereas no power in the other frequency bands in M1 in the low O_2 or recovery period was significantly different from that in the baseline period (P (low O_2, delta) $= 0.23$, $t_8 = 1.28$, $n = 9$ rats, one sample *t*-test *vs.* 1; P (low O_2, theta) $= 0.75$, $t_8 = 0.32$; P (low O_2, beta) $= 0.33$, $t_8 = 1.04$; P (low O_2, gamma) $= 0.44$, $t_8 = 0.80$; P (recovery, delta) $= 0.51$, $t_8 = 0.68$; P (recovery, theta) $= 0.40$, $t_8 = 0.88$; P (recovery, beta) $= 0.56$, $t_8 = 0.61$; P (recovery, gamma) $= 0.47$, $t_8 = 0.76$; Fig. 2B), suggesting that attenuation of motor cortical alpha power was recovered at least 20 min after termination of the experimental hypoxia. We also failed to find significant differences in the power in either frequency band in the low O_2 or recovery period for ACC (P (low O_2, delta) $= 0.35$, $t_8 = 0.98$, $n = 9$ rats, one sample *t*-test *vs.* 1; P (low O_2, theta) $= 0.89$, $t_8 = 0.15$; P (low O_2, alpha) $= 0.25$, $t_8 = 1.25$; P (low O_2, beta) $= 0.48$, $t_8 = 0.73$; P (low O_2, gamma) $= 0.69$, $t_8 = 0.41$; P (recovery, delta) $= 0.71$, $t_8 = 0.39$; P (recovery, theta) $= 0.47$, $t_8 = 0.76$; P (recovery, alpha) $= 0.33$, $t_8 = 1.03$; P (recovery, beta) $= 0.54$, $t_8 = 0.63$; P (recovery, gamma) $= 0.72$, $t_8 = 0.37$; Fig. 2C) or S1 (P (low O_2, delta) $= 0.16$, $t_8 = 1.52$, $n = 9$ rats, one sample *t*-test *vs.* 1; P (low O_2, theta) $= 0.91$, $t_8 = 0.12$; P (low O_2, alpha) $= 0.04$ ($>0.05/5$, Bonferroni correction), $t_8 = 2.42$; P (low O_2, beta) $= 0.62$, $t_8 = 0.52$; P (low O_2, gamma) $= 0.20$, $t_8 = 1.41$; P (recovery, delta) $= 0.38$, $t_8 = 0.93$; P (recovery, theta) $= 0.51$, $t_8 = 0.68$; P (recovery, alpha) $= 0.06$, $t_8 = 2.24$; P (recovery,

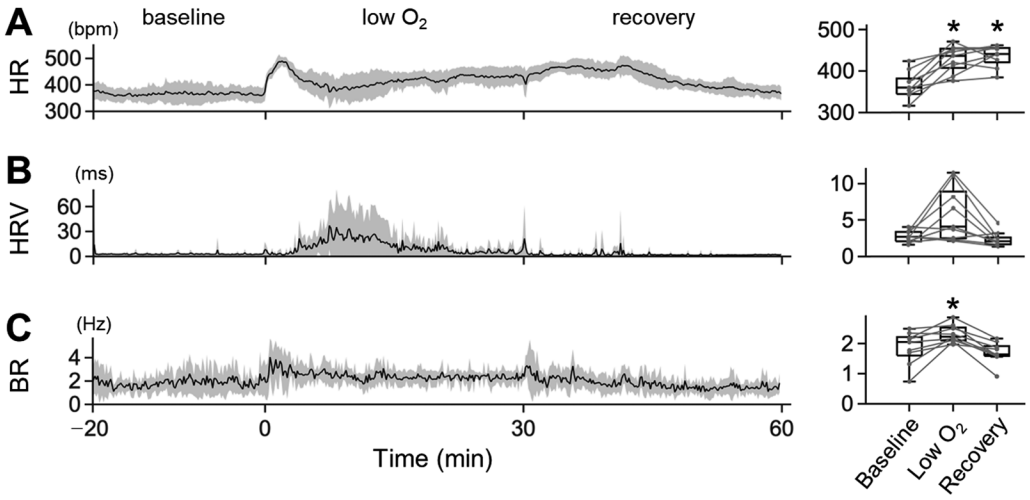

Fig. 3. Effects of Hypoxic Conditions on Cardiac and Breathing Activity

A, *Left*: Time course of HR (bpm) during the baseline, low O_2, and recovery periods. Data are presented as the mean (*black*) ± the standard deviation (*gray*) ($n = 9$ rats). *Right*: Comparison of HR among the baseline, low O_2, and recovery periods. **B**, Same as *A*, but for HRV. **C**, Same as *A*, but for BR. $*p < 0.05/3$ (note Bonferroni correction). *Abbreviations*: HR, heart rate; bpm, beats per minute; HRV, heart rate variability; BR, breathing rate.

beta) = 0.97, $t_8 = 0.04$; P (recovery, gamma) = 0.18, $t_8 = 1.47$; Fig. 2D). Thus, the low atmospheric oxygen attenuates LFP power possibly in a frequency- and region-specific manner.

In addition to neural signals, we further investigated whether and how cardiac, pulmonary, and motor functions were affected by the experimental hypoxia. Based on ECGs, we quantified HR and HRV in the three periods. We found that HR was significantly higher in the low O_2 and recovery periods than the baseline period (366 ± 33 bpm (baseline), 429 ± 32 bpm (low O_2), 436 ± 26 bpm (recovery); P (low O_2 *vs.* baseline) = 5.8×10^{-4}, $t_8 = 5.49$, $n = 9$ rats, paired *t*-test with *post-hoc* Bonferroni correction; P (recovery *vs.* baseline) = 5.9×10^{-4}, $t_8 = 5.47$; Fig. 3A). In contrast, RMSSD, an index of HRV, was not significantly affected by experimental hypoxia in either the low O_2 or recovery period, compared with the baseline period (2.68 ± 0.78 ms (baseline), 5.78 ± 3.72 ms (low O_2), 2.30 ± 1.00 ms (recovery); P (low O_2 *vs.* baseline) = 0.04 (>0.05/3), $t_8 = 2.54$, $n = 9$ rats, paired *t*-test followed by Bonferroni correction; P (recovery *vs.* baseline) = 0.33, $t_8 = 1.04$; Fig. 3B). Using EOGs, we evaluated respiratory functions and found that BR was significantly increased in the low O_2 period than the baseline period but returned to the baseline in the recovery period (1.86 ± 0.55 Hz (baseline), 2.31 ± 0.29 Hz (low O_2), 1.69 ± 0.36 Hz (recovery); P (low O_2 *vs.* baseline) = 1.5×10^{-2} (<0.05/3), $t_8 = 3.07$, $n = 9$ rats, paired *t*-test with Bonferroni correction; P (recovery *vs.* baseline) = 0.23, $t_8 = 1.31$; Fig. 3C). As for motor activity, the relative EMG amplitude in the low O_2 period was not significantly different from that in the recovery period (0.93 ± 0.42 (low O_2), 0.80 ± 0.22 (recovery); P (low O_2 *vs.* recovery) = 0.42, $t_7 = 0.85$, $n = 8$ rats, paired *t*-test). Moreover, each EMG amplitude was not significantly different from the baseline (P (low O_2) = 0.64 (>0.05/2), $t_7 = 0.49$ (low O_2), P (recovery) = 0.04 (>0.05/2), $t_7 = 2.49$ (recovery), $n = 8$ rats, one sample *t*-test *vs.* 1 with Bonferroni correction; Supplementary Fig. 2). These results confirmed that the effects of acute hypoxia were not confined to the brain.

DISCUSSION

In this study, we established an experimental system in which the oxygen concentration was controlled with the total air pressure constant. Using this system, we monitored neural activity in M1, S1, and ACC, and peripheral signals including ECGs, EOGs, and EMGs of rats while they were acutely exposed to less oxygen. We found that the power of alpha oscillations in M1 was reduced in response to low concentration of oxygen. Moreover, HR and BR were increased during the acute experimental hypoxia, after which the high HR was maintained. In contrast, HRV and EMG amplitude were neither increased nor decreased by the experimental hypoxia.

We found hypoxia-induced impairment of alpha oscillation power in M1, but a previous study reported that neocortical gamma power was suppressed during ventilatory depression in response to the severely hypoxic condition.[25] Our study is seemingly inconsistent with the previous report, but this discrepancy may be accounted for by the difference in brain regions from which neural activity was recorded. The anteroposterior coordinates used in our and their electrophysiological recordings are totally different, which in turn makes a difference in the brain regions affected by experimental hypoxia. In this sense, the alpha power reduction during hypoxia may be restricted in M1, although we cannot rule out the possibility that the acute hypoxia influences other frequency components of extracellular oscillations in regions except M1.

The plausible neural pathways responsible for the effects of hypoxia on neocortical activity may arise from the brainstem and terminate at M1 through the thalamus. Some medullary regions in the brainstem are chemoreceptive to the partial pressure of gases (*e.g.*, O_2 and CO_2) in blood; the nucleus tractus solitarius, C1 sympathoexcitatory region, and pre-Bötzinger complex are chemosensitive to hypoxia,[26,27] whereas the retrotrapezoid nucleus is sensitive to hypocapnia and hypercapnia.[28] Among them, for example, neurons in the nucleus of the solitary tract project to the ventral thalamic nucleus.[29] Ventral thalamic neurons further innervate the primary motor cortex.[30] Previous studies suggest that sensorimotor oscillations in rats originally initiates at the thalamus

based on the facts that thalamic rhythmic activity precedes cortical activity and that cortical activity is never generated in the absence of the thalamic activity.[31–33] In particular, cortical-projection neurons in the thalamus in rats generate burst firing during alpha-band sensorimotor rhythms,[32] implying that spiking activity of the thalamic neurons (projecting to the neocortex) contributes to alpha oscillations in M1 and S1. Thus, we presume that low atmospheric oxygen specifically modulates spiking activity in the ventral thalamus *via* the medulla oblongata, which in turn attenuates motor cortical alpha oscillations.

In addition to the neural activity, we demonstrate that some peripheral functions are influenced by the hypoxia. Based on our findings (Fig. 3), we propose that animals incorporate sufficient oxygen by increasing respiratory rate and HR when environmental oxygen is scarce (Figs. 3A, C). When the oxygen concentration returns to the baseline, BR returns to the original value (Fig. 3C), whereas HR maintains the higher value. These results suggests that after the hypoxic condition, sufficient oxygen is still quickly supplied to the tissue by high heartbeat, not by speeding up respiratory cycles, although we cannot rule out the possibility that the normal respiratory rate in the recovery period is compensated by increasing tidal volume. In contrast, RMSSD, which reflects vagally mediated changes in cardiac function,[24,34] is not affected by the hypoxic condition or environmental reoxygenation (Fig. 3B), suggesting almost no modulation of parasympathetic activity in response to environmental oxygen.

In general, compared to fossorial rodents such as naked mole rats,[35–37] most small rodents (including mice, rats, hamsters, and squirrels) in hypoxia either (i) exhibit panic-like escape behavior,[38] or (ii) search for colder environment, and reduce motor activity, huddling behavior, and body temperature (called anapyrexia) to conserve energy.[39–44] Consistent with the description, we indeed confirmed that rats attempted to escape the recording cage in the beginning of the low O_2 period. Nevertheless, the EMG amplitude in the low O_2 period was not so different from the baseline (Supplementary Fig. 2); we failed to observe obvious reduction in motor activity and reflex abstinence from energy consumptions.

Our electrophysiological recordings have revealed the central and peripheral responses to the lack of environmental oxygen. However, it is yet to be fully elucidated how these hypoxia-induced physiological changes are related to cognitive decline (or improvement), which is assessed by recording neural activity in the hippocampus and surrounding regions as well as the neocortex of animals engaging in behavioral tasks and sleeping before and after the tasks.[10,45] Moreover, although oxygen is supplied to the tissue by blood through blood vessels, how the physiological changes in this study are related to oxygen demands and delivery at the vascular level still remains unknown, which is indicated by parameters such as SpO_2, SaO_2, and PaO_2 based on blood gas analysis. In this light, monitoring of vascular and hematological parameters simultaneously with electrophysiological signals in freely moving animals at various concentrations of atmospheric oxygen will deepen our understanding of bodily responses to hypoxic and anoxic conditions and underscore the importance of sufficient oxygen for survival.

Acknowledgments This work was supported by JST ERATO (JPMJER1801), Institute for AI and Beyond of the University of Tokyo, and JSPS Grants-in-Aid for Scientific Research (18H05525, 20K15926).

Conflict of Interest The authors declare no conflict of interest.

Supplementary Materials This article contains supplementary materials.

REFERENCES

1) Arias-Reyes C, Soliz J, Joseph V. Mice and rats display different ventilatory, hematological, and metabolic features of acclimatization to hypoxia. *Front. Physiol.*, **12**, 647822 (2021).
2) Hayashi M, Nagasaka T. Hypoxic tachycardia in hypoxia-acclimated rats. *Jpn. J. Physiol.*, **32**, 149–152 (1982).
3) Murasato Y, Hirakawa H, Harada Y, Nakamura T, Hayashida Y. Effects of systemic hypoxia on R-R interval and blood pressure variabilities in conscious rats. *Am. J. Physiol.*, **275**, H797–H804 (1998).
4) Li G, Liu J, Guo M, Gu Y, Guan Y, Shao Q, Ma W, Ji X. Chronic hypoxia leads to cognitive impairment by promoting HIF-2α-mediated ceramide catabolism and alpha-synuclein hyperphosphorylation. *Cell Death Discov.*, **8**, 473 (2022).
5) Wang J, Xu Z, Xu L, Xu P. Inhibition of STAT3 signal pathway recovers postsynaptic plasticity to improve cognitive impairment caused by chronic intermittent hypoxia. *Sleep Breath.*, **27**, 893–902 (2023).
6) Akopyan NS, Baklavadzhyan OG, Karapetyan MA. Effects of acute hypoxia on the EEG and impulse activity of the neurons of various brain structures in rats. *Neurosci. Behav. Physiol.*, **14**, 405–411 (1984).
7) Okada S, Igata H, Sakaguchi T, Sasaki T, Ikegaya Y. A new device for the simultaneous recording of cerebral, cardiac, and muscular electrical activity in freely moving rodents. *J. Pharmacol. Sci.*, **132**, 105–108 (2016).
8) Sasaki T, Nishimura Y, Ikegaya Y. Simultaneous recordings of central and peripheral bioelectrical signals in a freely moving rodent. *Biol. Pharm. Bull.*, **40**, 711–715 (2017).
9) Shikano Y, Sasaki T, Ikegaya Y. Simultaneous recordings of cortical local field potentials, electrocardiogram, electromyogram, and breathing rhythm from a freely moving rat. *J. Vis. Exp.*, **2018**, 56980 (2018).
10) Yoshimoto A, Yamashiro K, Suzuki T, Ikegaya Y, Matsumoto N. Ramelteon modulates gamma oscillations in the rat primary motor cortex during non-REM sleep. *J. Pharmacol. Sci.*, **145**, 97–104 (2021).
11) Yoshimoto A, Yamashiro K, Ikegaya Y, Matsumoto N. Acute ramelteon treatment maintains the cardiac rhythms of rats during non-REM sleep. *Biol. Pharm. Bull.*, **44**, 789–797 (2021).
12) Yoshimoto A, Shibata Y, Kudara M, Ikegaya Y, Matsumoto N. Enhancement of motor cortical gamma oscillations and sniffing activity by medial forebrain bundle stimulation precedes locomotion. *eNeuro*, **9**, ENEURO.0521-21.2022 (2022).
13) Yamashiro K, Aoki M, Matsumoto N, Ikegaya Y. Polyherbal formulation enhancing cerebral slow waves in sleeping rats. *Biol. Pharm. Bull.*, **43**, 1356–1360 (2020).
14) Shibata Y, Yoshimoto A, Yamashiro K, Ikegaya Y, Matsumoto N. Delayed reinforcement hinders subsequent extinction. *Biochem. Biophys. Res. Commun.*, **591**, 20–25 (2022).
15) Karalis N, Sirota A. Breathing coordinates cortico-hippocampal dynamics in mice during offline states. *Nat. Commun.*, **13**, 467 (2022).
16) Kuga N, Nakayama R, Shikano Y, Nishimura Y, Okonogi T, Ikegaya

Y, Sasaki T. Sniffing behaviour-related changes in cardiac and cortical activity in rats. *J. Physiol.*, **597**, 5295–5306 (2019).
17) Liu J, Kashima T, Morikawa S, Noguchi A, Ikegaya Y, Matsumoto N. Molecular characterization of superficial layers of the presubiculum during development. *Front. Neuroanat.*, **15**, 662724 (2021).
18) Kudara M, Matsumoto N, Kuga N, Yamashiro K, Yoshimoto A, Ikegaya Y, Sasaki T. An open-source application to identify the three-dimensional locations of electrodes implanted into the rat brain from computed tomography images. *Neurosci. Res.*, **193**, 20–27 (2023).
19) Matsumoto N, Okamoto K, Takagi Y, Ikegaya Y. 3-Hz subthreshold oscillations of CA2 neurons *in vivo*. *Hippocampus*, **26**, 1570–1578 (2016).
20) Sato Y, Mizuno H, Matsumoto N, Ikegaya Y. Subthreshold membrane potential dynamics of posterior parietal cortical neurons coupled with hippocampal ripples. *Physiol. Int.*, **108**, 54–65 (2021).
21) Kudara M, Kato-Ishikura E, Ikegaya Y, Matsumoto N. Ramelteon administration enhances novel object recognition and spatial working memory in mice. *J. Pharmacol. Sci.*, **152**, 128–135 (2023).
22) Sato M, Matsumoto N, Noguchi A, Okonogi T, Sasaki T, Ikegaya Y. Simultaneous monitoring of mouse respiratory and cardiac rates through a single precordial electrode. *J. Pharmacol. Sci.*, **137**, 177–186 (2018).
23) Noguchi A, Matsumoto N, Morikawa S, Tamura H, Ikegaya Y. Juvenile hippocampal CA2 region expresses aggrecan. *Front. Neuroanat.*, **11**, 41 (2017).
24) Shaffer F, Ginsberg JP. An overview of heart rate variability metrics and norms. *Front. Public Health*, **5**, 258 (2017).
25) Fukushi I, Takeda K, Yokota S, Hasebe Y, Sato Y, Pokorski M, Horiuchi J, Okada Y. Effects of arundic acid, an astrocytic modulator, on the cerebral and respiratory functions in severe hypoxia. *Respir. Physiol. Neurobiol.*, **226**, 24–29 (2016).
26) Neubauer JA, Sunderram J. Oxygen-sensing neurons in the central nervous system. *J. Appl. Physiol.*, **96**, 367–374 (2004).
27) King TL, Heesch CM, Clark CG, Kline DD, Hasser EM. Hypoxia activates nucleus tractus solitarii neurons projecting to the paraventricular nucleus of the hypothalamus. *Am. J. Physiol. Regul. Integr. Comp. Physiol.*, **302**, R1219–R1232 (2012).
28) Guyenet PG, Stornetta RL, Souza GMPR, Abbott SBG, Shi Y, Bayliss DA. The retrotrapezoid nucleus: central chemoreceptor and regulator of breathing automaticity. *Trends Neurosci.*, **42**, 807–824 (2019).
29) Krout KE, Belzer RE, Loewy AD. Brainstem projections to midline and intralaminar thalamic nuclei of the rat. *J. Comp. Neurol.*, **448**, 53–101 (2002).
30) Lee C, Kim Y, Kaang B-K. The primary motor cortex: the hub of motor learning in rodents. *Neuroscience*, **485**, 163–170 (2022).
31) Semba K, Szechtman H, Komisaruk BR. Synchrony among rhythmical facial tremor, neocortical "alpha" waves, and thalamic non-sensory neuronal bursts in intact awake rats. *Brain Res.*, **195**, 281–298 (1980).
32) Hughes SW, Crunelli V. Thalamic mechanisms of EEG alpha rhythms and their pathological implications. *Neuroscientist*, **11**, 357–372 (2005).
33) Buzsáki G. The thalamic clock: emergent network properties. *Neuroscience*, **41**, 351–364 (1991).
34) Shaffer F, McCraty R, Zerr CL. A healthy heart is not a metronome: an integrative review of the heart's anatomy and heart rate variability. *Front. Psychol.*, **5**, 1040 (2014).
35) Ilacqua AN, Kirby AM, Pamenter ME. Behavioural responses of naked mole rats to acute hypoxia and anoxia. *Biol. Lett.*, **13**, 20170545 (2017).
36) Houlahan CR, Kirby AM, Dzal YA, Fairman GD, Pamenter ME. Divergent behavioural responses to acute hypoxia between individuals and groups of naked mole rats. *Comp. Biochem. Physiol. B Biochem. Mol. Biol.*, **224**, 38–44 (2018).
37) McNab BK. The metabolism of fossorial rodents: a study of convergence. *Ecology*, **47**, 712–733 (1966).
38) Fernandes GG, Frias AT, Spiacci A Jr, Pinheiro LC, Tanus-Santos JE, Zangrossi H Jr. Nitric oxide in the dorsal periaqueductal gray mediates the panic-like escape response evoked by exposure to hypoxia. *Prog. Neuropsychopharmacol. Biol. Psychiatry*, **92**, 321–327 (2019).
39) Steiner AA, Rocha MJA, Branco LGS. A neurochemical mechanism for hypoxia-induced anapyrexia. *Am. J. Physiol. Regul. Integr. Comp. Physiol.*, **283**, R1412–R1422 (2002).
40) Mortola JP, Feher C. Hypoxia inhibits cold-induced huddling in rat pups. *Respir. Physiol.*, **113**, 213–222 (1998).
41) Tattersall GJ, Milsom WK. Transient peripheral warming accompanies the hypoxic metabolic response in the golden-mantled ground squirrel. *J. Exp. Biol.*, **206**, 33–42 (2003).
42) Gordon CJ, Fogelson L. Comparative effects of hypoxia on behavioral thermoregulation in rats, hamsters, and mice. *Am. J. Physiol.*, **260**, R120–R125 (1991).
43) Steiner AA, Branco LGS. Hypoxia-induced anapyrexia: implications and putative mediators. *Annu. Rev. Physiol.*, **64**, 263–288 (2002).
44) Dzal YA, Jenkin SEM, Lague SL, Reichert MN, York JM, Pamenter ME. Oxygen in demand: How oxygen has shaped vertebrate physiology. *Comp. Biochem. Physiol. A Mol. Integr. Physiol.*, **186**, 4–26 (2015).
45) Matsumoto N, Kitanishi T, Mizuseki K. The subiculum: unique hippocampal hub and more. *Neurosci. Res.*, **143**, 1–12 (2019).